Anal Bioanal Chem (2011) 400:1347–1358
DOI 10.1007/s00216-011-4872-z

ORIGINAL PAPER

Hydrodynamic and electrical considerations in the design of a four-electrode impedance-based microfluidic device

Gusphyl Justin · Mansoor Nasir · Frances S. Ligler

Received: 17 January 2011 / Revised: 28 February 2011 / Accepted: 3 March 2011 / Published online: 30 March 2011

Abstract A four-electrode impedance-based microfluidic device has been designed with tunable sensitivity for future applications to the detection of pathogens and functionalized microparticles specifically bound to molecular recognition molecules on the surface of a microfluidic channel. In order to achieve tunable sensitivity, hydrodynamic focusing was employed to confine the electric current by simultaneous introduction of two fluids (high- and low-conductivity solutions) into a microchannel at variable flow-rate ratios. By increasing the volumetric flow rate of the low-conductivity solution (sheath fluid) relative to the high-conductivity solution (sample fluid), increased focusing of the high-conductivity solution over four coplanar electrodes was achieved, thereby confining the current during impedance interrogation. The hydrodynamic and electrical properties of the device were analyzed for optimization and to resolve issues that would impact sensitivity and reproducibility in subsequent biosensor applications. These include variability in the relative flow rates of the sheath and sample fluids, changes in microchannel dimensions, and ionic concentration of the sample fluid. A comparative analysis of impedance measurements using four-electrode versus two-electrode configurations for impedance measurements also highlighted the advantages of using four electrodes for portable sensor applications.

Keywords Hydrodynamic focusing · Impedance spectroscopy · Nyquist plot · Bode impedance · Bode phase · Microfluidics

Introduction

The benefits of utilizing microfluidic systems in analysis have already been highlighted in the literature and include small sample or reagent volumes, high throughput, low fabrication costs, small footprint, rapid analysis times, and high sensitivity [1]. Laminar flow, a characteristic behavior of fluids in motion within channels of micron-sized dimensions, can be an advantage or disadvantage, depending on the intended operation. In microsystems, convective mixing of two or more fluids simultaneously introduced into the microchannel does not occur, as in the case of macroscale systems. When two fluids enter a microfluidic channel, they flow side by side without any eddies normally associated with turbulent flow (multi-stream laminar flow). The primary mechanism of mixing is diffusion between the two streams, and as long as low Reynolds numbers are maintained, convective mixing is minimal.

In the microfluidic regime, hydrodynamic focusing can be used not only to position one flow stream using another but also to control the dimensions (cross-sectional areas) of two or more fluids simultaneously introduced into a microfluidic channel (multi-stream laminar flow) by altering their relative flow rates. By increasing the flow rate of one fluid relative to a second fluid, the cross-sectional area of the channel occupied by the faster flowing fluid will be greater than that occupied by the slower moving fluid. There is minimal convective mixing as long as the Reynold's numbers associated with the flow through the channel are low. Hydrodynamic focusing of rectangular reactive streams has been used for patterning

Electronic supplementary material The online version of this article (doi:10.1007/s00216-011-4872-z) contains supplementary material, which is available to authorized users.

G. Justin · M. Nasir · F. S. Ligler (✉)
Center for Bio/Molecular Science and Engineering,
U.S. Naval Research Laboratory,
4555 Overlook Avenue SW,
Washington, DC 20375, USA
e-mail: frances.ligler@nrl.navy.mil

surfaces [2], while Hasenbank et al. [3] used such a multi-stream laminar flow system to investigate heterogeneous electrochemical processes within a microchannel. Computational simulations of electrochemical processes in the presence of multi-stream laminar flows in microfluidic devices have also been performed [4].

Hydrodynamic focusing is also an effective means of using multi-stream laminar flow for the creation of a virtual microfluidic channel with soft, compliant boundaries. One example is a modified Coulter counter to measure the sizes of particles. Rodriguez-Trujillo et al. [5] demonstrated counting of 20-μm polystyrene microparticles using both optical microscopy and impedance detection methods. They focused a rectangular stream 2 μm wide×50 μm high within a microchannel 190 μm wide and 50 μm high using three inlet streams—a sample fluid stream (comprising a high-conductivity fluid) flanked by two focusing fluid streams (deionized water). Using this approach, they demonstrated confinement of the focused sample stream in width, but the height of the focused stream was dictated by the physical height of the microchannel. Coplanar microelectrodes in contact with the high-conductivity sample stream were used to measure the impedance of the particles as they passed within the vicinity of the generated electric field, but the sensitivity of the counter was constrained by the height of the channel.

Bernabini et al. [6] also fabricated a modified Coulter counter device for the impedance-based detection and discrimination of smaller particles, 1 and 2 μm in diameter. In order to enhance sensitivity, two pairs of parallel electrodes (one pair situated in the ceiling aligned with the other in the floor of the microchannel) were used to measure the change in the solution resistance between the electrodes as particles were transported through the center of the microchannel via the focused stream. The authors were able to create a focused stream 12 μm wide by 30 μm high, with the height determined by the physical height of the microchannel and the width determined by the relative flow rate of the faster flowing focusing fluids. Discrimination of particles of differing dimensions was determined based on a scatter plot of the particle transient time through the electric fields versus the magnitude of the electrical signal response at a specific frequency (503 kHz). As in the Rodriquez-Trujillo paper, the channels were kept wide (though not high) to limit clogging from complex real-world samples. Hydrodynamic focusing of a high-conductivity fluid (phosphate-buffered saline) with a low-conductivity sheathing fluid (deionized water) [5] or oil/surfactant mixture [6] was used to reduce the cross-sectional area of the conducting fluid and increase sensitivity.

Impedance-based techniques have long been used for the detection of bacteria [7–12]. However, these studies were based on a two-electrode impedance model, employing either single frequency or multi-frequency analysis. Four-electrode impedance spectroscopy has been used for monitoring changes in the extracellular conductivity of cell monolayers [13]. Studies performed by Hua and Pennell [14] have demonstrated the use of a four-electrode impedance method for the detection of physically entrapped 20-μm diameter mammalian epithelial cells within a 17-μm-high by 125-μm-wide channel. Laugere et al. [15] proposed that at low-frequency ranges, the impedance effects associated with the electrode–solution interface (double-layer capacitance, Warburg diffusion effects, and electron transfer resistance) can be effectively reduced or eliminated when a four-electrode (two impedance sense electrodes and two current source electrodes) system is utilized instead of the more common two-electrode configuration. Four-electrode systems predominantly measure changes that occur in the bulk solution impedance (see Electronic supplementary material (ESM) Fig. S1). Cells are essentially insulating at low frequencies [16], that is, at frequencies less than the characteristic frequency of a cell (2–3 MHz) [7]. As a consequence, changes in the bulk solution conductivity with the introduction of the insulating cells can be detected as a change in impedance or admittance [14]. A four-electrode configuration for AC impedance measurements can measure very low impedances [17]. This configuration is therefore particularly important for developing low-cost electronic systems based on absolute impedance ($|Z|$) measurements of the conducting fluid path, where the electrode–solution interfacial impedance changes can be ignored.

A microfluidic biosensor based on four-electrode impedance detection and hydrodynamic focusing for tunable sensitivity was recently reported by our group with the goal of achieving high sensitivity as well as high detection specificity with the introduction of real-world complex samples (Fig. 1a) [18, 19]. Tunable sensitivity was achieved using hydrodynamic focusing to confine the current (Fig. 1b), while antibody immobilization between the impedance sensing electrodes permitted high specificity for the target cells (Fig. 1a). Increasing the flow-rate ratio of the focusing fluid (in this case, also called the sheath fluid) to the sample fluid increased confinement of the current to the detection region and thus increased sensitivity to the particles (conducting microparticles and cells) present between the electrodes [18, 19]. One of the primary limitations of the work described previously by Rodriguez-Trujillo et al. [5] and Bernabini et al. [6] is the lack of target specificity. Impedance-based systems such as the modified Coulter counters described by these two groups may be used to discriminate target particles or cells based on size, but these systems would not differentiate between two different particles of similar size. To overcome this challenge, the device described previously by our

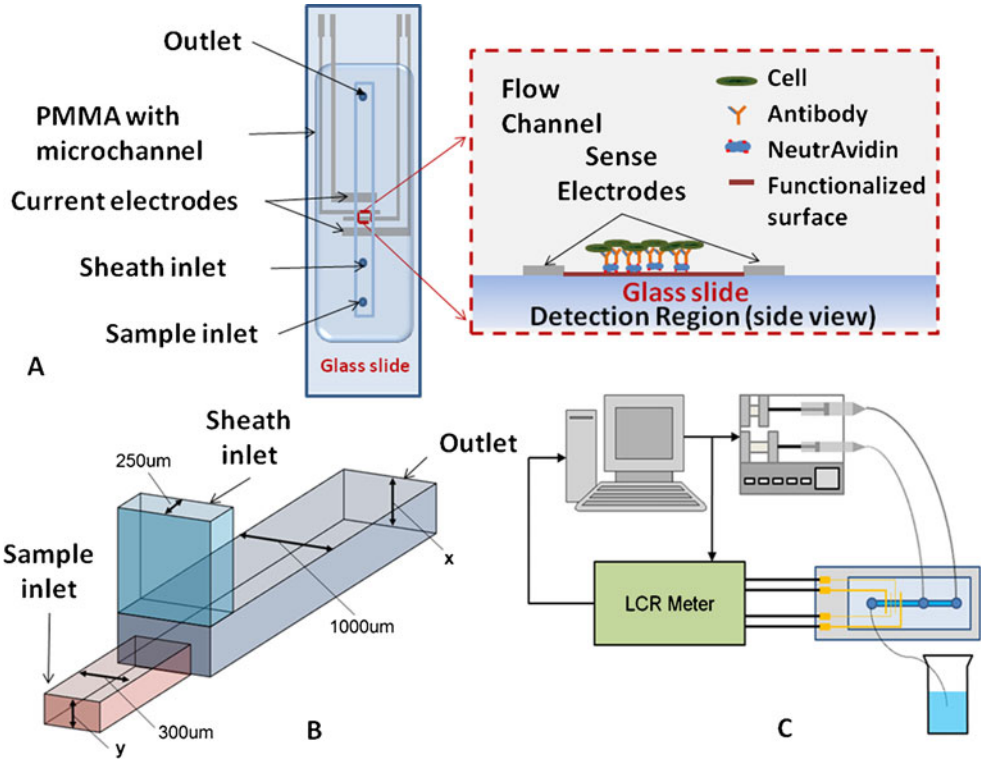

Fig. 1 **a** Assembled microfluidic device and detection region. **b** Hydrodynamic focusing employing a vertical input for the sheath fluid and a narrower horizontal input microchannel for the sample fluid (inlet height, y=150 μm; channel height, x=250 μm). **c** Instrumentation for impedance measurement under flow conditions

group would be capable of discriminating cells through specific antibody capture at the surface of the microchannel between the coplanar electrodes. Detection would be based on changes in the impedance of the conducting path between the impedance sense electrodes generated by the bound cells or particles (Fig. 1a). The height and width of that conducting path would be determined by hydrodynamic focusing. The primary purpose of this paper, however, was not to demonstrate detection but to examine the numerous factors—in particular the electrical and hydrodynamic factors—that can adversely impact detection, leading to lack of reproducibility in our novel system.

A major challenge to detection, however, is in achieving adequate sensitivity. For previous electrical measurements in microfluidic systems, the sensitivity and limits of detection have been closely related to the dimensions of the microchannel. Greatest sensitivity is achieved by minimizing the cross-sectional area of the conducting fluid stream relative to that of the cell or particle. Impedance-based detection systems are often sensitive to a number of systemic parameters that can compromise the sensitivity of the device. It is important to be able to differentiate the miscellaneous background from the detection response, but there are significant challenges associated with this discrimination. Differentiating background noise from an actual detection event can be difficult, and it becomes important to identify the various factors that can lead to a false positive. Variability in parameters, such as (1) relative flow rates of sheath to sample, (2) microchannel dimensions, and (3) the ionic concentration of the sample stream, can impact impedance-based detection, particularly during hydrodynamic focusing at high flow-rate ratios. In order to achieve consistent detection, the variability in each of these parameters must be minimized as each can have an appreciable impact on the magnitude of the impedance measurements.

In this study, an analysis of the four-electrode impedance microfluidic device developed by our group is performed in an effort to optimize the device and to resolve issues impacting sensitivity and reproducibility for future biosensor applications, including variability in the relative flow rates of the sheath and sample fluids, changes in microchannel dimensions, and ionic concentration of the sample fluid. A comparative analysis of impedance measurements using four- versus two-electrode configurations is also performed to highlight the advantage of using four electrodes for portable biosensor applications.

Experimental

Electrode patterning and microfluidic system fabrication

Glass microscope slides (25×75×1 mm, Daigger, Vernon Hills, IL, USA) were cleaned according to the procedure described by Cras et al. [20] using a 1:1 methanol (MeOH)/hydrochloric acid (HCl) mixture for 30 min, followed by concentrated sulfuric acid (H_2SO_4) solution for 30 min and rinsing in deionized (DI) water. The platinum electrodes were fabricated using standard photolithographic techni-

ques. The fabrication procedure has previously been described [18, 19]. Briefly, the electrodes were patterned onto the glass slides using an NR7 1000PY negative photoresist. An ABM, Inc. Mask Aligner (Scotts Valley, CA, USA) was used for mask alignment and exposure. A base thin layer of Ti (0.03 μm) was first deposited on to the slides followed by platinum (0.15 μm) using electron beam evaporation (Temescal Model FC-2000 E-Beam Evaporator). The photoresist was removed by brief ultrasonication in acetone. The inner two "sense electrodes" were separated by a distance of 500 μm and were slightly smaller in width (500 μm) than the two outer current-source electrodes (1,000 μm).

Electrode enclosure within a microfluidic chamber was achieved by adhering a polymethyl methacrylate (PMMA) block with a milled microchannel (main channel, 250 μm high × 1,000 μm wide; inlet channel, 150 μm high × 300 μm wide) to the surface of the glass slides using either UV polymerizable glue (Norland Products #72, Cranbury, NJ, USA) or ARcare™ 8890 double-sided tape (Adhesives Research, Glen Rock, PA, USA). The differing widths of the inlet and main microchannel provided a simple means to create a dome-shaped focused stream confined in both the vertical (z) and horizontal (y) directions during hydrodynamic focusing. A detailed description of the device fabrication has been published previously [18, 19].

Impedance spectroscopy and hydrodynamic focusing

Impedance analyses of the devices were based on both two-electrode and four-electrode single- and multi-frequency impedance setups. Electrical impedance spectroscopy of the patterned glass substrate was performed using an Agilent 4284 LCR meter (Santa Clara, CA, USA), interfaced via a data acquisition board and LabView software (National Instruments, Austin, TX, USA; Fig. 1c). A frequency range of 100 Hz to 1 MHz was used. Single-frequency measurements were made at 1 kHz. A dual-syringe pump (Pump 33, Harvard Apparatus, Holliston, MA, USA) was also controlled with LabView for dual-inlet hydrodynamic focusing. For the four-electrode system, a sinusoidal signal (10-mV peak-to-peak potential, 0-V offset potential) was applied between the two outer current source electrodes, while the two inner sensing electrodes were used for impedance interrogation of the focused sample stream. For the two-electrode configuration, the same sinusoidal voltage signal was applied between the two inner electrodes, while the outer current electrodes were left open. In order to perform two-electrode impedance measurements using the LCR meter, the low current (Lcurr) and low potential (Lpot) leads were shorted, while the high current (Hcurr) and high potential (Hpot) leads were shorted. The same electrode pair used for impedance sensing in the four-electrode configuration was therefore used to make the two-electrode impedance measurements.

Finite element analysis

Simulations for flow and concentration distribution in the microchannels were performed using the COMSOL Multiphysics package (COMSOL Inc., Palo Alto, CA, USA). The symmetry of the channel about the width dimension made it possible to simulate only half of the channel and reduce computation times. The simulations were conducted

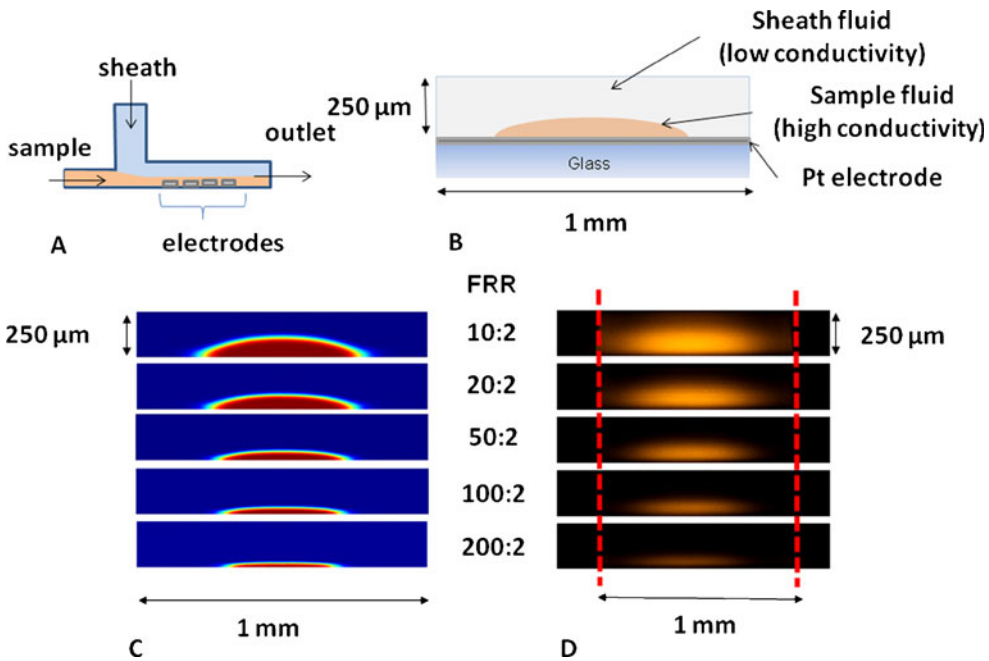

Fig. 2 **a** Partial side view of microchannel (not drawn to scale) indicating direction of sheath, sample, and outlet flows during hydrodynamic focusing. **b** Microchannel cross-section indicating the focused stream (sample fluid) over a platinum electrode on glass slide. **c** Finite element analysis simulations in COMSOL of flow-rate ratios. **d** Confocal microscopy images of sample stream (water with rhodamine dye) under varying flow-rate ratios

in two steps. In the first step, Navier–Stokes equations were solved for steady, incompressible flow with zero-slip boundary condition on the channel walls. The sheath and sample flows were specified to be fully developed at their respective inlets. The volumetric flow rates were also halved in each case to comply with the channel symmetry condition. In the second step, the convective and diffusive transport of species was simulated based on the results of the flow simulation. The solute concentration distributions were found assuming a diffusion coefficient of 1×10^{-9} m^2 s^{-1}, which is typical of low-molecular-weight solutes [21]. The presence of the conducting ions in the fluid dictated the initial solute concentration values of 1 and 0 for sample and sheath streams, respectively. An automesh with tetrahedral elements was used for all simulations. In order to accurately resolve the mass transport along the interface between the sheath and sample streams, adaptive meshing was used to increase the mesh density in subsequent simulations. The mesh refinement process was repeated until the results were no longer found to depend on mesh density (h-method). Sheath and sample fluids were simulated as water at room temperature (20 °C) with density and dynamic viscosity as 1×10^3 kg m^{-3} and 1×10^{-3} N sm^{-2}, respectively. Furthermore, it was assumed that the inclusion of conducting ions in the sample fluid did not change the fluid density and viscosity; therefore, the only factors affecting the distribution of the model species were diffusion and convection. The details of the multiphysics modules and the equations used to define flow and mass transport characteristics have been previously described [18].

Confocal microscopy

Visualization of concentration distributions under flow focusing conditions in the microchannel were performed using a Nikon Eclipse TE2000-E inverted microscope equipped with a Nikon D-Eclipse C1si confocal spectral imaging system (Nikon, Japan). A region roughly 10 mm downstream from the sheath and sample stream T-junction was imaged. Deionized water was used for both streams with FWT Red Powder fluorescent dye (Bright Dyes, Miamisburg, OH, USA) added only to the sample fluid for visualization of the focused stream. A dual-syringe pump (Harvard Apparatus Model 33) was used to flow the sheath and sample fluids at desired flow rates. Confocal microscopy was performed using a 10× objective (NA 0.45, WD 4.00 Dry). Image resolution was 512×512 pixels, with a *Z*-step size spacing of 10 μm and a pixel dwell time of 7.46 ms. A 40-mW argon laser (wavelength 514 nm) was used for excitation. Appropriate filter sets were used to collect fluorophore emissions from the dye between 583 and 593 nm. The spectral detector gain was set accordingly to provide a sharp contrast of the focused stream. The scanned slices for each *Z*-step were combined to create a three-dimensional volume using the NIS-Elements AR confocal image processing software (Nikon).

Results and discussion

Hydrodynamic focusing

In order to attain tunable sensitivity in the microfluidic device, hydrodynamic focusing was employed to create a virtual microchannel that functions as an adjustable aperture for confining current. The electric current confinement within this virtual microchannel is due to the differing conductivities between the sample stream (high-conductivity phosphate-buffered saline solution) and the sheath stream (low-conductivity deionized water). For greatest sensitivity, it is ideal to create a focused stream with as small a cross-sectional area and volume as possible. This requires both vertical and horizontal constriction of the focused stream which would normally require three sheathing inlets, as described by Bernabini et al. [6].

The greater the number of inlets, however, the greater the background noise associated with fluctuations in the focused stream dimensions during impedance interrogation from sources such as pump pulsations, microbubble movements, or tubing compression. To reduce the number of inlet sheath streams, the microchannel was fabricated so that a dome-shaped focus stream could be produced (Fig. 2). To achieve this, a smaller channel (150 μm high×300 μm wide) originating from the sample inlet was fabricated which opened into a larger main channel (250 μm high×1,000 μm wide). The sheath inlet entered the junction at a right angle to the sample and main channels and had a width similar to that of the main channel (Figs. 1b and 2a). As a consequence, the faster moving sheath fluid surrounded the sample fluid as it exited the inlet microchannel, forcing constriction of the fluid in both the vertical (*z*) and horizontal (*y*) directions. Both the height and base width of the dome-shaped focused fluid could be reduced by increasing the flow-rate ratio, that is, the ratio of the input volumetric flow rate of the sheath fluid to that of the sample fluid.

Figure 2b is a schematic that shows a cross-section (through the microchannel, an electrode, and the glass substrate) of the focused sample stream as it was confined. Finite element analysis simulations in COMSOL (Fig. 2c) as well as confocal microscopy images (Fig. 2d) demonstrated that constriction of the virtual microchannel in terms of both the height and width of the focused stream occurred when the sheath-to-sample flow-rate ratio was increased. As the focused sample stream was confined further and

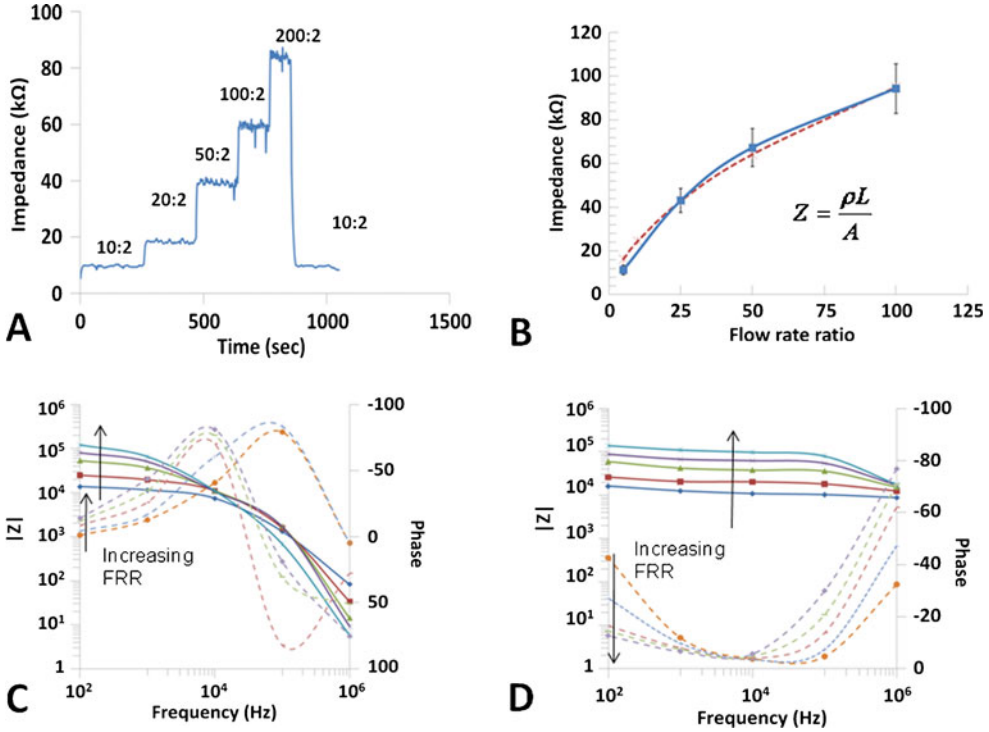

Fig. 3 Effect of hydrodynamic focusing on impedance: **a** Impedance responses (10 mV p-p, at 1-kHz frequency) from Pt chip associated with step increases in the flow-rate ratios of the sheath (DI water) to the sample (PBS) fluids. **b** Comparison between experimental impedance values (*solid line*) and theoretical impedance values (*dashed line*). Theoretical impedance was determined based on the focused stream cross-sectional areas in Table 1. Length of the conducting stream, L, was taken as the distance between the sense electrodes (0.5 mm) and resistivity, ρ, taken as 62.9 Ωcm [22]. Resistivity, length, and cross-sectional area were substituted into Eq. 1. **c** Four-electrode Bode impedance (*solid lines*) and phase plots (*dashed lines*) associated with hydrodynamic focusing. **d** Two-electrode Bode impedance (*solid*) and phase (*dashed*) plots associated with hydrodynamic focusing. Measurements were made at 10^2, 10^3, 10^4, 10^5, 10^6 Hz. Flow rate ratios were 10, 20, 50, 100, and 200 μL/min (sheath) to 2 μL/min (sample). *Arrows* indicate direction of increased hydrodynamic focusing

further, the surface area of the electrodes exposed to the high-conductivity sample stream was also slightly reduced due to the decrease in the width of the sample stream. Figure 2c, d also suggests that some diffusional mixing between the sample and sheath streams can occur. This would be expected, particularly since both fluids are water-based and ions in the sample fluid can diffuse across the laminar flow boundary. Diffusion during hydrodynamic focusing has previously been discussed in detail by Nasir et al. [19].

Effect of relative sheath-to-sample flow rates on single- and multi-frequency impedance

For the given physical dimensions of the microchannel, as well as the flow-rate ratios involved in hydrodynamic focusing, the height, base width, and cross-sectional area of the focused stream were predicted based on the finite element model used to simulate this process (Table 1). Table 1 shows that as the relative flow rate of the sheath to the sample stream increased, the height, base width, and cross-sectional area of the dome-shaped focused stream decreased. From the predicted cross-sectional area, one can also predict the associated impedance for the conducting path spanning the distance between the impedance sense electrodes of the coplanar four-electrode configuration. It is the change in impedance within this region that is most important for target detection (Fig. 1a). Impedance is inversely proportional to the cross-sectional area (A) of the conductive path and directly proportional to the electrode separation distance (L), which can be approximated by:

$$Z = \frac{\rho L}{A} \tag{1}$$

where Z is the solution impedance, ρ is the resistivity (62.9 Ωcm for phosphate-buffered saline solution) [22], L is the length of the conducting path (500 μm between the sense electrodes), and A is the cross-sectional area of the conducting path (values obtained from Table 1). Figure 3a shows the change in impedance with increasing sheath flow rates of 10, 20, 50, 100, and 200 μL/min and a constant 2-μL/min sample flow rate. The sample flow rate of 2 μL/min was used because it was the smallest flow rate that could be reliably generated by the syringe pump with a 250 μL

Table 1 Theoretical dimensions of dome-shaped focused sample streams at five different flow rate ratios based on COMSOL simulations

Sheath (μL/min)	Sample (μL/min)	Flow-rate ratio	Height (μm)	Width (μm)	Area ($\times 10^{-4}$ cm^2)
10	2	5	103	564	1.93
20	2	10	77	502	1.28
50	2	25	50	440	0.73
100	2	50	36	414	0.49
200	2	100	24	414	0.33

syringe. The increase in the impedance was expected as the cross-sectional area of the focused stream decreased with increased flow-rate ratio (Fig. 2 and Table 1). Therefore, as the sample fluid was increasingly confined, the cross-sectional area of the conducting fluid stream, as well as the surface area of the electrodes exposed to the conducting solution, decreased. In Fig. 3a, one can also notice that the signals were rather noisy. This background noise in the impedance signal measurements was a reflection of fluctuations in the dimensions of the conducting stream, largely resulting from pulsatile flow from the syringe pumps. The mismatch in the pulsatile flow of the sheath and sample streams entering the microfluidic channel—particularly at the highest flow-rate ratios—caused variability in the cross-sectional area of the focused stream over time and consequent variability in the impedance. For sensor applications, it is important to keep this background noise to a minimum as the sensitivity of the device could be reduced due to the masking of small signals from low concentrations of target cells or particles.

Figure 3b indicates that the impedance predicted by Eq. 1 was consistent with the experimental values. Three separate channels were used, and as a consequence, the relatively large standard deviations may reflect slight variations in the dimensions of the milled microchannels, which would consequently affect the dimensions of the focused stream and the exposed surface area of the electrodes.

Shown in Fig. 3c, d are Bode impedance and phase plots obtained using four-electrode and two-electrode configurations, respectively, with frequencies ranging from 100 Hz to 1 MHz. Both configurations demonstrated an increase in $|Z|$ with focusing at low to medium frequency. At low frequency, the phase for the four-electrode configuration shifted to more negative values with increased focusing, but to more positive values for the two-electrode configuration. The phase information obtained using a four-electrode configuration is fundamentally different from that obtained using two-electrode systems. In the four-electrode system, the phase should reflect the capacitive behavior of the bulk

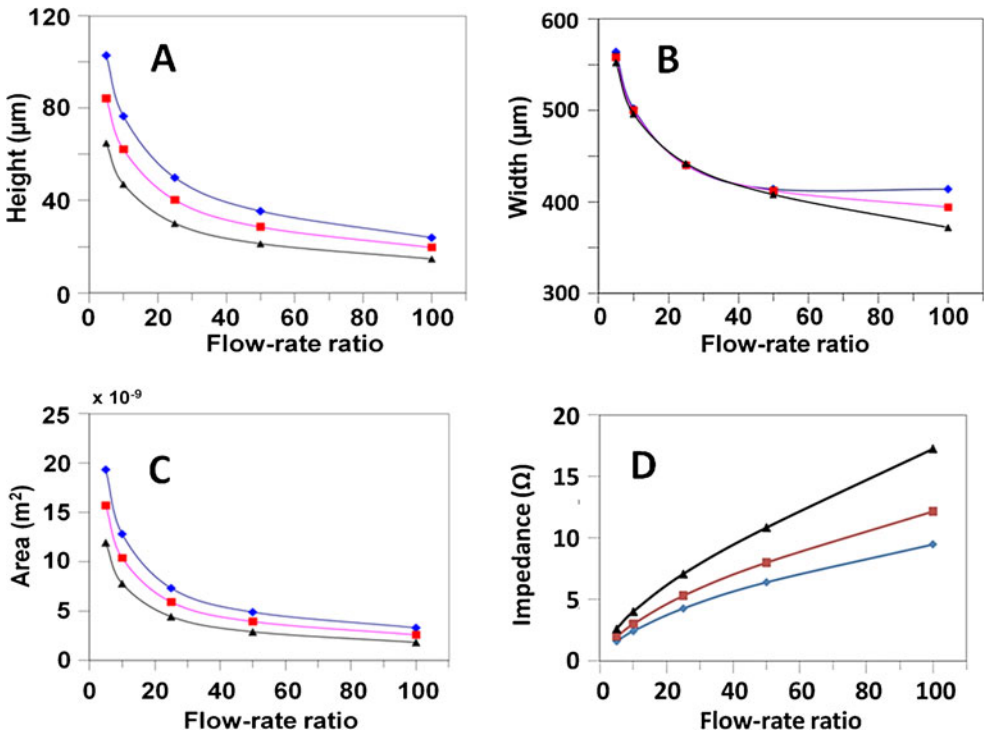

Fig. 4 Changes in height (**a**), base width (**b**), cross-sectional area (**c**), and impedance (**d**) of a dome-shaped focused stream at variable flow rate ratios and microchannel heights. The effect of the differing physical height of the microchannel becomes amplified at higher flow-rate ratios. Flow-rate ratios of 5, 10, 25, 50, and 100 were used. Channel heights were 150 μm (*triangle*), 200 μm (*square*), and 250 μm (*dimond*)

solution. However, the phase information for four-electrode systems is generally not well understood, and a detailed treatment is beyond the scope of this paper. The increasingly negative phase values for the two-electrode system at low frequencies are a direct indication of changes occurring at the electrode–electrolyte interface. The plot is informative in that it indicates that the area of the electrode surface in contact with the electrolyte (phosphate-buffered saline, PBS) is decreasing, particularly at low frequencies. A shrinking electrode surface area (A) will result in a decreasing double-layer capacitance (C), in accordance with the following equation:

$$C = \frac{\varepsilon_o \varepsilon_r A}{d} \tag{2}$$

where ε_o is the permittivity of free space (8.85×10^{-12} F/m), ε_r is the relative permittivity of the solution, and d represents the Debye length. This equation produces trends that support the results illustrated in Fig. 2c, d, namely that confinement of the base width of the virtual dome-shaped microchannel is occurring.

Increasing $|Z|$ for the four-electrode configuration with hydrodynamic focusing shows that the bulk resistance of the focused conducting stream increases with decreasing cross-sectional area (Fig. 3a). Distortion of both $|Z|$ and phase at the higher frequencies for the four-electrode system have been previously described and explained by Hsieh and colleagues as due to a voltage divider effect associated with high contact resistances. Low frequencies (≤1 kHz) are optimal when using a four-electrode impedance detection system. The low-frequency measurements are beneficial to our detection system since cells are insulating at low frequencies, which would result in a larger impedance response.

The height, base width, and the cross-sectional area of hydrodynamically focused sample streams for different microchannel heights (main channel) were determined using finite element simulations of the fluidic device in COMSOL. Figure 4 shows that as the height of the microfluidic channel increases, the height, width, and cross-sectional area of the focused stream also increase. The base width of the dome-shaped focus stream does not decrease very much until the highest flow-rate ratio used (100). The result is that the impedance increases (Fig. 4d), in accordance with Eq. 1, with increasing flow-rate ratio. This is an important point which should be taken into consideration, particularly during the course of an impedance interrogation experiment that utilizes hydrodynamic focusing. High flow rates within the microchannel, which may be necessary to achieve small focused streams, have the potential to create sufficient pressures within the channel to alter the physical dimensions of the microchannel. If polydimethylsiloxane (PDMS) or other soft, compliant materials are used for the fabrication of the microchannel, the dimensions can more easily be altered. This was one of the reasons governing the decision to use PMMA instead of PDMS. If PMMA is used, gluing or

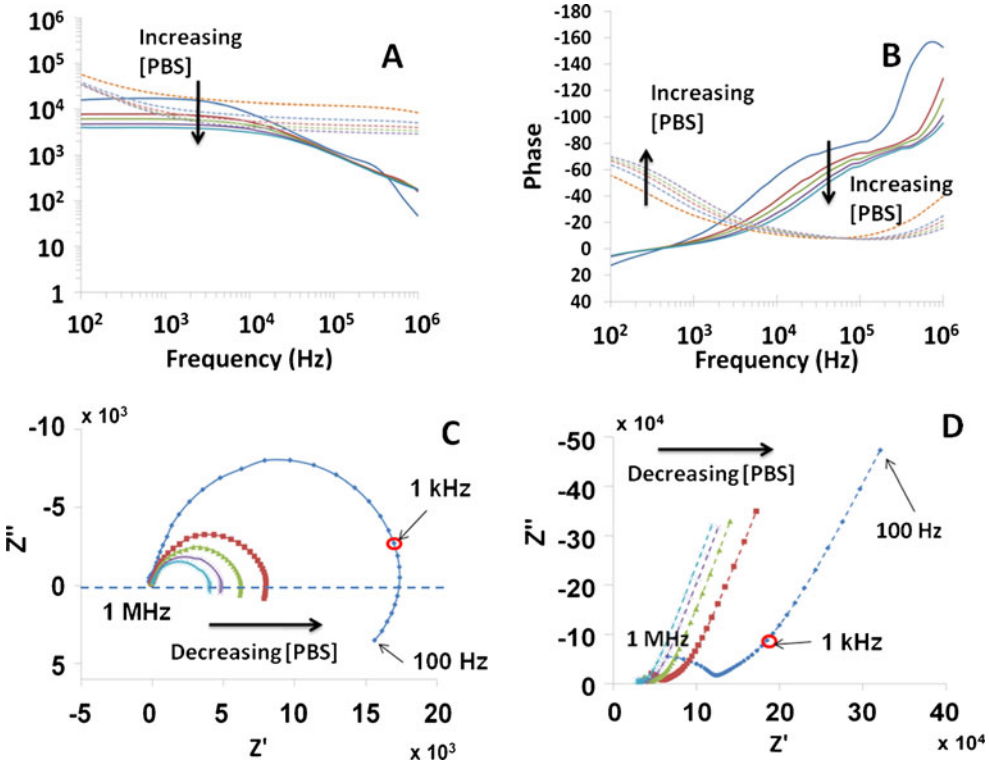

Fig. 5 Bode impedance (**a**) and phase (**b**) plots for two-electrode (*dashed lines*) and four-electrode (*solid lines*) impedance spectroscopy data acquired for varying PBS ionic concentrations (0.2×, 0.4×, 0.6×, 0.8×, and 1×). In both the two- and four-electrode systems, decreasing impedance is associated with increasing ionic concentration. The entire channel was filled with PBS and there is no hydrodynamic focusing. Nyquist impedance plots for four-electrode (**c**) and two-electrode (**d**) systems are shown

adhesive tape is necessary to bond the PMMA to the glass slides bearing the electrodes. High pressures within the microchannel may not deform the PMMA, but could cause expansion of the adhesive, resulting in an increase of the microchannel height by a few microns. From the results in Fig. 4d, we see that a 50-μm change in the physical height of the microchannel can translate to an impedance change of more than 20 kΩ at the highest flow-rate ratio, which should provide the greatest sensitivity for detection. A tenth of that change, ~5 μm, could be extrapolated to cause an impedance change of almost 2 kΩ, still a relatively large number if a few micron-sized cells or particles are to be detected. One solution would be to make simultaneous measurements from two pairs of sense electrodes (detection and reference pair in addition to the two current electrodes) in order to obtain differential impedance measurements of the target analyte impedance versus background, but the pairs must be fabricated to be identical in all dimensions, which is also not guaranteed.

Effect of ionic concentration on impedance

Electrical impedance spectroscopy (EIS) of the microfluidic device was performed using both two- and four-electrode configurations with five PBS concentrations ranging from 0.2× to 1×. All EIS measurements in this instance were made in the absence of hydrodynamic focusing within the microfluidic device. As expected, an increase in the absolute impedance, $|Z|$, was observed with decreasing ionic strength (Fig. 5a) for both the two- and four-electrode configurations. At the lowest frequencies, the impedance change associated with the changing ionic concentrations was greater for the four-electrode system than for the two-electrode system. This was not unexpected as the two-electrode system measures changes at the electrode–solution interface while the four-electrode system measures changes in the bulk solution properties. Within the medium- to high-frequency range (>10 kHz), the two-electrode system demonstrated impedances similar to that of the four-electrode system in the lower frequency range (<10 kHz) across all PBS concentrations. At higher frequencies, the two-electrode system measures the bulk resistance properties (as indicated by the fact that the four-electrode low frequency $|Z|$ is comparable to the two-electrode high frequency $|Z|$).

In Fig. 5b, the influence of the solution concentration and conductivity on phase is illustrated. At low frequencies, there was little change to the phase for the four-electrode system compared to the two-electrode system. However, at higher frequencies, there were large changes in phase for the four-electrode system, with phase moving toward more positive values with increasing PBS concentration. In the two-electrode system, the phase tended to more negative values with increasing PBS concentration. The increasing ionic strength is associated with an increase in the relative permittivity of the solution [23], leading to an increase in the capacitance (see Eq. 2). The low-frequency phase measurements in the two-electrode system reflected the changing capacitive property of the electrode with ionic strength.

Figure 6 shows how a change in solution ionic concentration can resemble the expected sensitivity enhancement of our microfluidic system to a detected microparticle or cell. Two concentrations, 0.8× and 1.0× PBS, were used as the sample fluid and impedance measurements were made using flow rates of 10, 20, 50, 100, and 200 μL/min (sheath) to 2 μL/min (sample). There was an expected increase in impedance from 1.0× to 0.8× PBS due to the decrease in ionic strength (Fig. 6a). However, the impedance change (ΔZ) increased with increased focusing (Fig. 6b) up to a sheath sample flow-rate ratio of 100 to 2. The effect of changing ionic concentrations on the sensitivity of the device is an issue that must be considered for applications involving complex real-world samples. For continuous impedance monitoring, changes in ionic concentration can affect the sensitivity by masking the effect associated with the presence of cells.

Electrical impedance spectroscopy using two- and four-electrode configurations

EIS was used to determine factors that can influence the impedance measurements during a detection event as well

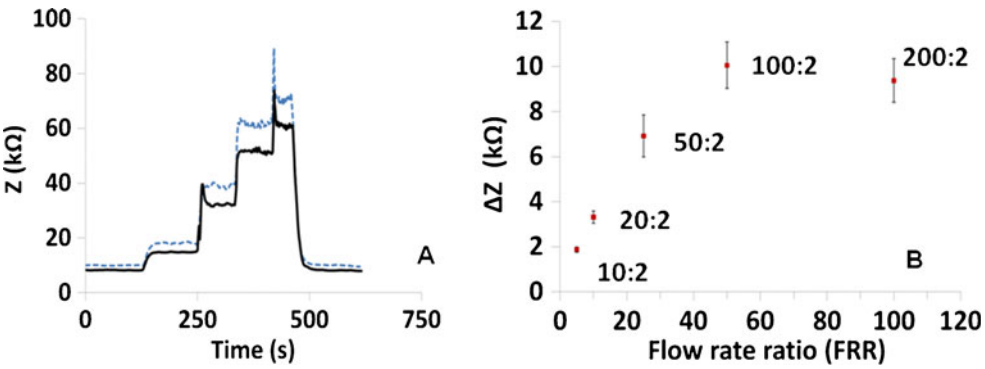

Fig. 6 Effect of changing ionic concentration of the sample stream from 0.1× (*solid line*) to 0.8× (*dashed line*) PBS on impedance during hydrodynamic focusing at flow rate ratios of 10, 20, 50, 100, and 200 μL/min (sheath) to 2 μL/min (sample). **a** Raw data for impedance. **b** Difference in impedance between 0.8× and 1.0× PBS

as to determine the optimal frequency for impedance-based detection. This approach was also used to help elucidate the differences between two- and four-electrode configurations in such sensors. As mentioned previously, an advantage of four-electrode configurations for such impedance measurements is that the effect of electrode polarization at low (near DC) frequencies is not an issue, unlike the case for two-electrode systems. Detection systems that employ two-electrode configurations measure impedance changes that occur when cells bind to the electrode surface. The presence of the cells alters the interfacial properties of the electrode–solution interface (capacitance, charge transfer resistance, Warburg impedance; see ESM Fig. S1), and the interfacial effects become particularly apparent at very low frequencies. Therefore, it is important to be able to eliminate the observation of impedance changes due to nonspecific adsorption at the electrode surfaces. The two-electrode configuration is not ideal for situations where the bulk solution properties (including resistance and capacitance) are investigated and low frequencies are required. In the microfluidic device described here, the four-electrode impedance configuration is ideal. Only target cell binding in the detection region between the electrodes should cause a change in the impedance between the sense electrodes, while the system should be insensitive to changes at the electrode interface (see Fig. 1a).

The Bode impedance plot in Fig. 5a showed that at low frequencies (<10 kHz), the absolute impedance ($|Z|$) remained relatively constant for the four-electrode system, but increased with decreasing frequency for the two-electrode configuration. The Bode phase plot (Fig. 5b) revealed that at lower frequencies, the phase became more negative for the two-electrode system. This indicated the capacitive behavior associated with the polarization of the electrodes for two-electrode impedance measurements. In the case of four-electrode systems, however, this capacitive behavior of the electrodes is not significant; therefore, the effects of electrode polarization on four-electrode impedance are not a concern. The fact that the phase for the four-electrode configuration approaches zero at the lowest frequencies suggests that resistive behavior is being measured by this system. The resistance measured is that of the bulk solution.

The Nyquist plots for the four- and two-electrode configurations were very different (Fig. 5c, d). The four-electrode system (Fig. 5c) produced semicircular plots that were consistent with the behavior of an RC-parallel circuit (solution resistance and capacitance), while the two-electrode configuration (Fig. 5d) revealed a dominating linear behavior at low frequencies. In the four-electrode Nyquist graph, the resistance and capacitance that contribute to the semicircular plots both reflect bulk solution properties inherent to Z' and Z''. This is different from the two-electrode Nyquist plot where the imaginary component, Z'', is largely attributable to the electrode double-layer capacitance as well as Warburg diffusion effects (electrode–solution interfacial properties). These data further support the use of a four-electrode system for the low-frequency impedance detection of cells.

The Bode impedance plots in Fig. 5a, b indicate that the 1-kHz interrogation frequency is appropriate for discriminating measurements of solutions of variable impedance while not too low to elicit electrochemical reactions at the current electrodes during long-term measurements. Electrochemical reactions during low-frequency (near DC) measurements at the current electrodes may affect the local solution conductivity and shorten the life span of the electrodes due to corrosion. In the presence of hydrodynamic focusing, however, the constant flow through the microchannel may contribute to the removal of the reaction products; therefore, local solution conductivity changes may not be a significant issue during impedance interrogation.

Very low frequencies in the four-electrode configuration used with our system also appear to elicit positive Z'', normally associated with inductive effects (Fig. 5c). Inductance is generally not observed in electrochemical systems, and therefore, the result is unexpected. However, a recent study identified four-electrode impedance configurations as strongly susceptible to cell geometry and experimental conditions [24]. The authors attributed the inductive arc to the voltage divider effect that was previously reported by Hsieh et al. [25]. To avoid any of the ill effects associated with low or high frequencies in this system, the 1-kHz measurement frequency appeared to be a reasonable choice for four-electrode impedance interrogation. However, since an impedance change associated with cell detection is sought, the actual impedance values associated with the system become less important.

It should be noted that for the development of a portable microfluidic biosensor device, the electronics used for impedance interrogation should be small, inexpensive, and relatively simple to use. For detection systems that would be used to detect a bacterial species, and perhaps even provide quantitation or size discrimination, a numerical value in the form of a voltage measurement is sufficient. The actual implementation of a four-electrode impedance-based microfluidic biosensor may not be able to perform frequency sweeps as can be performed in the laboratory setting using more expensive and sophisticated equipment such as an LCR meter or potentiostat/impedance analyzer. As a consequence, there is a need to measure the voltage drop across the two sense electrodes in the four-electrode system at a single low frequency, where that voltage drop is representative of the impedance change in the bulk solution and not reflective of impedance changes at the electrode surfaces themselves. This can theoretically be done using a simple instrument such as a voltmeter or a simple voltage-

to-current converter circuit, and a current source to supply the desired current at the interrogating frequency. Such instrumentation for voltage measurements has previously been described [5, 6, 18].

Conclusions

A microfluidic device that utilizes four-electrode impedance in conjunction with hydrodynamic focusing for tunable sensitivity has been characterized for future use as a system for cell detection. Hydrodynamic focusing of a high-conductivity sample stream with a low-conductivity sheath stream allows tunable sensitivity through current confinement within a virtual microfluidic channel with soft boundaries that is less susceptible to clogging than small rigid channels. Increasing the flow-rate ratio increases the measured impedance due to the reduction in the cross-sectional area of the virtual channel (the focused stream). The impedance is inversely proportional to the cross-sectional area of the focused stream, following Eq. 1. Impedance measurements offer a highly sensitive technique for target detection; however, this sensitivity is subject to factors including the physical dimension of the microchannel, the dimensions of the focused conducting stream, and the ionic conductivity. The four-electrode configuration is ideal for simple implementations of low impedance measurements, resulting from its insensitivity to electrode polarization. For future applications involving the detection of cells, which are insulating at low frequencies, the four-electrode impedance should provide greater sensitivity and reliability than two-electrode configurations for monitoring changes within the detection region. Although the two-electrode configuration is capable of measuring bulk solution impedance at higher frequencies, these higher frequencies would be less sensitive to the presence of cells. The measurement of low-frequency impedance of the bulk solution (impedance changes in the conductive path between the sense electrodes) is best performed using the four-electrode system.

Acknowledgments The authors would like to thank Lisa Shriver-Lake, Lenny Tender, Rachel Snider, Brett Martin, Scott Trammell, Walter Dressick, and Christopher Spillmann at the Naval Research Laboratory for their suggestions in this manuscript. Gusphyl Justin and Mansoor Nasir were National Research Council (NRC) Postdoctoral Fellows. The research was funded by the Defense Threat Reduction Agency. The views are those of the authors and do not reflect opinion or policy of the US Navy or Department of Defense.

References

1. Whitesides GM (2006) The origins and the future of microfluidics. Nature 442(7101):368–373
2. Takayama S, McDonald JC, Ostuni E, Liang MN, Kenis PJA, Ismagilov RF, Whitesides GM (1999) Patterning cells and their environments using multiple laminar fluid flows in capillary networks. PNAS 96(10):5545–5548
3. Hasenbank MS, Fu E, Nelson JB, Schwartz DT, Yager P (2007) Investigation of heterogeneous electrochemical processes using multi-stream laminar flow in a microchannel. Lab Chip 7(4):441–447
4. Santillo MF, Ewing AG, Heien ML (2011) Trends in computational simulations of electrochemical processes under hydrodynamic flow in microchannels. Anal Bioanal Chem 399:183–190
5. Rodriguez-Trujillo R, Mills C, Samitier J, Gomila G (2007) Low cost micro-Coulter counter with hydrodynamic focusing. Microfluid Nanofluid 3(2):171–176
6. Bernabini C, Holmes D, Morgan H (2011) Micro-impedance cytometry for detection and analysis of micron-sized particles and bacteria. Lab Chip 11:407–412. doi:10.1039/C0LC00099J
7. Gawad S, Schild L, Renaud P (2001) Micromachined impedance spectroscopy flow cytometer for cell analysis and particle sizing. Lab Chip 1(1):76–82
8. Ruan C, Yang L, Li Y (2002) Immunobiosensor chips for detection of *Escherichia coli* O157:H7 using electrochemical impedance spectroscopy. Anal Chem 74(18):4814–4820
9. Wu J, Ben Y, Chang H-C (2005) Particle detection by electrical impedance spectroscopy with asymmetric-polarization AC electroosmotic trapping. Microfluid Nanofluid 1(2):161–167
10. Varshney M, Li Y, Srinivasan B, Tung S (2007) A label-free, microfluidics and interdigitated array microelectrode-based impedance biosensor in combination with nanoparticles immunoseparation for detection of *Escherichia coli* O157:H7 in food samples. Sens Actuators B 128(1):99–107
11. Yang L, Li Y, Erf GF (2004) Interdigitated array microelectrode-based electrochemical impedance immunosensor for detection of *Escherichia coli* O157:H7. Anal Chem 76(4):1107–1113
12. Yang L, Li Y, Griffis CL, Johnson MG (2004) Interdigitated microelectrode (IME) impedance sensor for the detection of viable *Salmonella typhimurium*. Biosens Bioelectron 19(10):1139–1147
13. Asfour H, Soller W, Posnack N, Pollard A, Kay M (2010) Low frequency impedance spectroscopy of cell monolayers using the four-electrode method. J Phys Conf Ser 224:012085. doi:10.1088/1742-6596/224/1/012085
14. Hua SZ, Pennell T (2009) A microfluidic chip for real-time studies of the volume of single cells. Lab Chip 9:251–256
15. Laugere F, Guijt RM, Bastemeijer J, van der Steen G, Berthold A, Baltussen E, Sarro P, van Dedem GWK, Vellekoop M, Bossche A (2003) On-chip contactless four-electrode conductivity detection for capillary electrophoresis devices. Anal Chem 75:306–312
16. Geddes L, Baker L (1967) The specific resistance of biological material—a compendium of data for the biomedical engineer and physiologist. Med Biol Eng Comput 5(3):271–293
17. Deslouis C, Musiani M, Tribollet B, Vorotyntsev M (1995) Comparison of the AC-impedance of conducting polymer-films studied as electrode-supported and freestanding membranes. J Electrochem Soc 142(6):1902–1908
18. Nasir M, Ateya DA, Burk D, Golden JP, Ligler FS (2010) Hydrodynamic focusing of conducting fluids for conductivity-based biosensors. Biosens Bioelectron 25(6):1363–1369
19. Nasir M, Price DT, Shriver-Lake LC, Ligler F (2010) Effect of diffusion on impedance measurements in a hydrodynamic flow focusing sensor. Lab Chip 10(20):2787–2795
20. Cras JJ, Rowe-Taitt CA, Nivens DA, Ligler FS (1999) Comparison of chemical cleaning methods of glass in preparation for silanization. Biosens Bioelectron 14(8–9):683–688
21. Culbertson CT, Jacobson SC, Michael Ramsey J (2002) Diffusion coefficient measurements in microfluidic devices. Talanta 56 (2):365–373

22. Johnson AM, Sadoway DR, Cima MJ, Langer R (2005) Design and testing of an impedance-based sensor for monitoring drug delivery. J Electrochem Soc 152(1):H6–H11
23. Rica RA, Jiménez ML, Delgado AV (2010) Electric permittivity of concentrated suspensions of elongated goethite particles. J Colloid Interface Sci 343(2):564–573
24. Lvovich V, Smiechowski M (2009) AC impedance investigation of conductivity of automotive lubricants using two- and four-electrode electrochemical cells. J Appl Electrochem 39(12):2439–2452
25. Hsieh G, Ford SJ, Mason TO, Pederson LR (1997) Experimental limitations in impedance spectroscopy: part VI. Four-point measurements of solid materials systems. Solid State Ionics 100:297–311